# Investigating the Dynamic Behavior of Hardox Plates under Shockwave Loading

**Shaygan Shahed Haghighi**
*M.Sc. Student of Vehicle Dynamical Systems Research Laboratory, School of Automotive Engineering, Iran University of Science and Technology, Narmak, Tehran, Iran*

**Javad Marzbanrad**[1]
*Professor, Vehicle Dynamical Systems Research Laboratory, School of Automotive Engineering, Iran University of Science and Technology, Narmak, Tehran, Iran*

## Abstract
Hardox wear-resistant steels are widely used in applications involving extreme impact and abrasion conditions. This study investigates the dynamic behavior and deformation mechanisms of Hardox plates subjected to intense shockwave loading. The key objectives are to characterize the performance of Hardox steels under high strain rate events and develop predictive models using finite element analysis and machine learning approaches. Controlled shockwave experiments provide insights into the relationships between charger parameters and the resulting pressure impulses imposed on Hardox specimens. Finite element simulations in LS-DYNA enable virtual testing across a wide range of loading intensities. The models reveal how factors like peak incident pressure and impulse duration influence the extent of plate deflection and potential for material failure. A Random Forest regression model demonstrates promising accuracy in predicting maximum dynamic deflection of Hardox plates using blast characteristics and plate thickness as features. This data-driven approach can assist designers in optimizing the thickness and supports of Hardox components intended for extreme impact applications. Overall, the study enhances fundamental understanding of the mechanisms influencing the penetrative and damage tolerance of quenched and tempered wear-resistant steels under shockwave loading across high strain rates.

**Keywords**: Hardox wear-resistant steel, Shockwave loading, Random Forest regression, High strain rates analysis.

1-Corresponding Author

## Introduction

Hardox wear-resistant steels have become indispensable materials for applications involving severe impact, abrasion, and extreme loading conditions. Studying the performance characteristics of these steels under high-intensity dynamic events is crucial for several reasons.
First, Hardox steels are extensively used in mining, construction, transportation, and military equipment that undergo punishing in-service conditions. These include rock crushing hammers, truck bodies, loader buckets, armored vehicles, and more. Understanding the behavior of Hardox steels in response to shockwave loading and high-velocity impacts is vital for determining their survivability and damage tolerance under such extreme conditions [1].

Second, research on dynamic effects is essential for the design and maintenance of Hardox components. The ability to accurately model and predict deflections, penetrations, and failure modes allows engineers to optimize the thickness, joining, and support structures to prevent premature fatigue or sudden fracture [2-3]. Likewise, science-based inspection criteria can be developed by correlating the residual life of Hardox parts with surface deformation, cracking, or brinelling caused during intense loading events.

Finally, investigations under controlled test conditions provide new insights into the fundamental mechanisms of how strain rate, hydrostatic stresses, adiabatic shear, and microstructural phases influence the penetration and damage resistance of these materials [4,5]. The physics-based understanding and experimental data can be used to improve manufacturing processes, refine material models, and develop next-generation Hardox alloys with even higher impact toughness or performance under shockwave loading.

The key objectives of this research are to:

1) Characterize the performance of Hardox wear-resistant steel plates when subjected to extreme shockwave loading conditions representative of high intensity impacts.

2) Utilize controlled experiments and finite element simulations to gain insights into the dynamic response, deformation modes, and potential failure mechanisms of Hardox steels under impulsive loading scenarios.

3) Develop predictive models using machine learning approaches to estimate the deflection and damage tolerance of Hardox plates based on blast parameters.

4) Establish science-based criteria and guidelines for the design and analysis of Hardox components intended for applications involving severe impacts or blast loading.

The significance of this work lies in furthering the fundamental understanding of hardened steel behavior under high strain rate events. The data and analytical framework developed can assist engineers in optimizing the thickness, support design, and integrity of Hardox parts to resist intense impacts and shocks. The findings will aid material selection, life prediction, and damage assessment of components made from these wear-resistant steels.

This paper is structured as follows. Section 2 surveys the mechanical properties and composition of different Hardox steel grades. Section 3 details the shockwave loading experiments and simulation parameters. Finite element modeling methodology and results are covered in Section 4. Section 5 explains the machine learning approach for predicting dynamic plate deflections. Finally, Section 6 presents the key conclusions and recommendations for future work.

## Performance Characteristics of Hardox Steels

Hardox steels possess unique properties that make them well-suited for applications involving high strain rates and extreme dynamic loading conditions. The exceptional hardness, strength, and toughness of these wear-resistant steels enable them to withstand intense impacts and high dynamic loading.

The high hardness of Hardox steels, ranging from 400 to over 650 HBW depending on the grade, provides excellent resistance to abrasion and contact damage. Surface hardness in excess of 600 HBW for premium grades like Hardox 600 and Extreme enables them to resist erosive wear even under heavy cyclic loading. The hardness is attributed to

the tempered martensitic microstructure produced by quenching and tempering. This imparts substantial strength and limits plastic deformation during impact events.
The mechanical properties of different types of Hardox steels are shown in table 1.

**Table 1- Mechanical Properties[6]**

| Hardox Plate Type | Wear Resistance | Toughness (Impact Energy) | Hardness (HBW) |
|---|---|---|---|
| Hardox HiTuf | Moderate | 40 J / -40 °C | 310-370 |
| Hardox 400 | Good | 45 J / -40 °C | 370-430 |
| Hardox 450 | Better | 50 J / -40 °C | 390-475 |
| Hardox 500 | High | 37 J / -40 °C | 470-540 |
| Hardox 550 | Higher | 30 J / -40 °C | 525-575 |
| Hardox 600 | Very High | ~30 J / -40 °C | 570-640 |
| Hardox Extreme | Extremely High | ~40 J / -40 °C | 650-700 |

In addition to hardness, Hardox steels exhibit very high yield and tensile strengths on the order of 1000-1600 MPa. The strength provides damage tolerance under dynamic loads by inhibiting crack initiation and propagation. The precise control of alloying elements like manganese and chromium allows combining high hardness with good fracture toughness.

**Table 2- Chemical Composition [6]**

| Hardox Plate Type | C(max %) | Si (max %) | Mn (max %) | P(max %) | S(max %) | Cr (max %) | Ni (max %) | Mo (max %) | B(max %) |
|---|---|---|---|---|---|---|---|---|---|
| **Hardox HiTuf** | 0.2 | 0.6 | 1.6 | 0.05 | 0.02 | 0.7 | 2 | 0.7 | 0.005 |
| **Hardox 400** | 0.32 | 0.7 | 1.6 | 0.025 | 0.01 | 2.5 | 1.5 | 0.6 | 0.004 |
| **Hardox 450** | 0.26 | 0.7 | 1.6 | 0.025 | 0.01 | 1.4 | 1.5 | 0.6 | 0.005 |
| **Hardox 500** | 0.3 | 0.4 | 1.3 | 0.02 | 0.01 | 2.2 | 2 | 0.4 | 0.005 |
| **Hardox 550** | 0.44 | 0.5 | 1.3 | 0.02 | 0.01 | 1.4 | 1.4 | 0.6 | 0.004 |
| **Hardox 600** | 0.47 | 0.7 | 1.5 | 0.015 | 0.01 | 1.2 | 2.5 | 0.7 | 0.005 |
| **Hardox Extreme** | 0.47 | 0.5 | 1.4 | 0.015 | 0.01 | 1.2 | 2.5 | 0.8 | 0.005 |

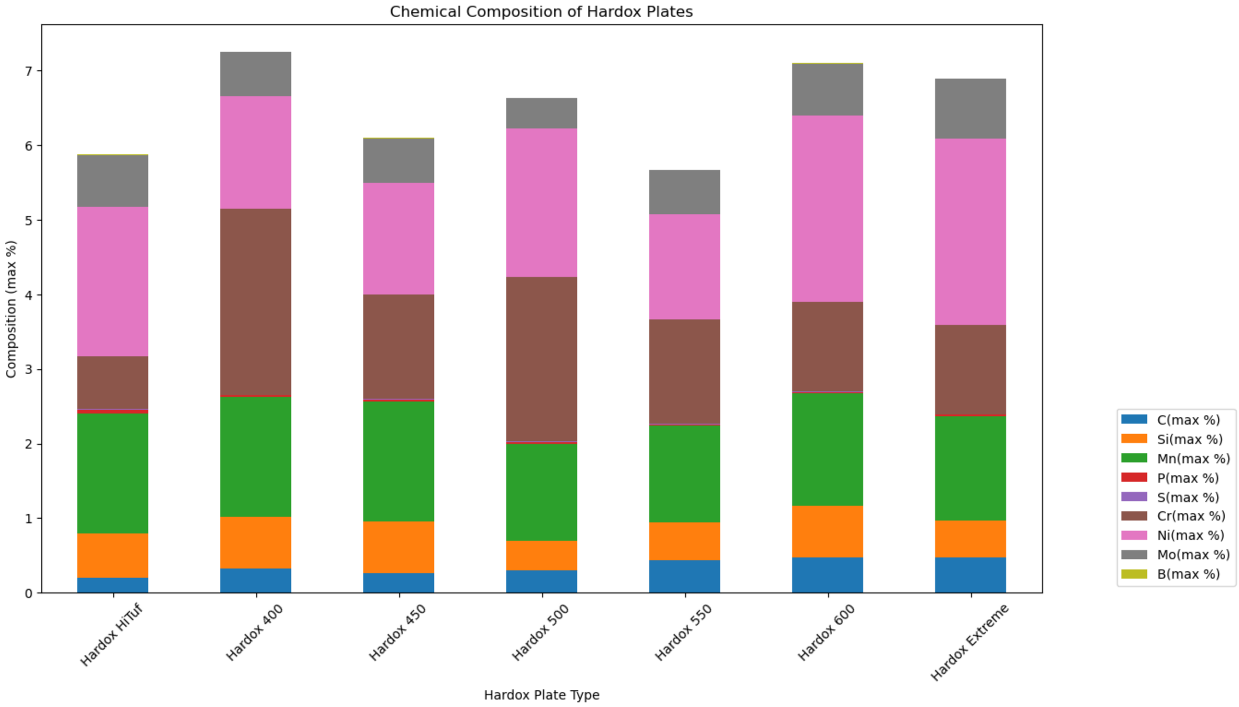


**Figure (1) Chemical Composition of Different Hardox Plate Types**

According to the tables provided, the following observations can be made regarding the relationship between the chemical composition of different Hardox steel plates and their mechanical properties:
Carbon plays an important role in determining the hardness, wear resistance, and tensile strength of Hardox steel plates. The highest content of carbon is found in Hardox Extreme and Hardox 600, both of which increase in hardness and wear resistance as their carbon content increases. In spite of the fact that higher carbon content increases hardness and tensile strength, it can negatively affect welding properties, plasticity, and toughness[7]. Recent research investigated the influence of carbon and nitrogen on the microstructure, mechanical properties, wear resistance, and corrosion resistance of Cr, Mn, Fe, Co, Ni alloys with high entropy. Both carbon and nitrogen were found to be part of the face-centered cubic solid solution, contributing to precipitate formation. As a result of the presence of these substances, yield and ultimate tensile strength were increased, while ductility was decreased[8].
Numerous research articles have examined the effects of silicon on the mechanical properties of steel. Silicon enhances steel's strength[9], hardness[10], heat resistance[11], and oxidation resistance[12], [13], but may adversely affect its machinability. In order to achieve the desired properties, the amount of silicon can be controlled[14]. Liu et al examined the microstructural evolution of HT-9 steels used to clad advanced nuclear reactors as a function of silicon content and tempering temperature in a study. It was found that a higher silicon content was correlated with a higher yield strength, tensile strength, and plasticity. Increasing the tempering temperature reduces strength and hardness, but increases plasticity and toughness[15].
All types of Hardox steel have a relatively consistent manganese content, suggesting it is a fundamental component of its properties. The addition of manganese to steel is often used to improve its strength, hardness, as well as wear resistance. Furthermore, there is a study by MOOR et al that examines the effects of carbon and manganese modifications on the quenching and partitioning properties of CMnSi steels. Measurements of the tensile properties and austenite retention percentage of different grades of steel were conducted[16].
A low level of phosphorus (P) and sulfur (S) is present in Hardox steel, probably due to the fact that high levels can leave steel susceptible to brittleness[17]. There is a slight decrease in phosphorus content as hardness and wear resistance increase.

Alloying elements such as chrome (Cr), nickel (Ni), and molybdenum (Mo) improve steel's mechanical properties. Strength is increased by molybdenum[18], toughness is increased by nickel[19], and hardness and wear resistance are enhanced by chrome[20].
Boron is relatively consistent across all types of steel. Boron is often added to steel to increase its hardness and strength[21].

In summary, the exceptional hardness, strength, and fine-grained microstructure of Hardox steels enable them to resist penetration, absorb shockwave energy, and prevent crack propagation under dynamic loads. The uniformity of their properties improves reliability when subjected to intense impacts. These characteristics justify further research into the behavior of Hardox steels under severe loading conditions relevant for high wear applications.

**Exploring Shockwave-Induced Impulses in Hardox Plates**

The shockwave loading experiments utilized explosive charges to generate high-amplitude pressure pulses to load the Hardox test specimens. As the detonation products rapidly expand, a shock front forms and compresses the surrounding air. The interaction of this blast wave with the Hardox plate surface leads to a reflected shock wave that imposes intense impulsive pressures on the order of multiple megabars [22,23].

The shockwave loading on the plates can be characterized by several key parameters - peak incident pressure, impulse duration, and total impulse imparted. As the initial shock front impacts the plate, the reflected pressure can reach up to 2-8 times the incident pressure due to the impedance mismatch between air and steel [24,25]. Pressure transducers mounted near the plate surface capture the reflected pressure profile during the shockwave loading event.

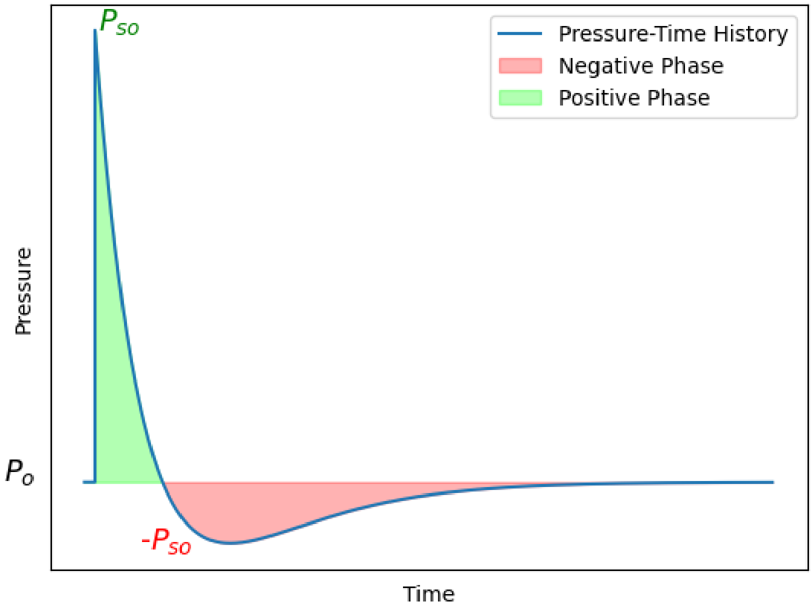


**Figure (2) Shockwave Pressure-Time history**

Figure 2 illustrates a typical pressure-time curve of a blast wave. When the blast wave reaches a certain point, the pressure jumps to a maximum of overpressure, $P_{so}$, above the normal atmospheric pressure, $P_o$. The pressure then drops to the ambient level and then goes below the ambient level to a negative pressure $-P_{so}$ (creating a suction effect) before returning to the average level. The term $P_{so}$ is often used to describe the peak side-on overpressure, incident peak overpressure, or simply peak overpressure. The pressure-time curve has two main phases: the part above the ambient level is called the positive phase, and the part below the ambient level is called the negative phase. The negative phase lasts longer and has lower intensity than the positive phase. As the distance from the explosion increases, the duration of the positive-phase blast wave also increases, resulting in softer and longer shock pulses. Charges that are very close to a target structure apply a very high and sudden pressure load on a small area of the structure; charges that are farther away apply a lower and longer pressure load on the whole structure. The blast wave covers the entire structure, with reflection and diffraction effects creating complex focusing patterns and shadow zones around the structure [23].
Behind the shock front is a blast wind moving at supersonic velocity that imparts impulse to structures. Shockwaves reflect and reinforce when impacting surfaces, subjecting materials to short duration impulses reaching over 20 MPa in certain scenarios. The high strain rates imposed on materials by shockwave loading, on the order of 104 s-1, necessitate analysis using dynamic material models [26].

To study the effects of shockwave parameters on Hardox plates, the research utilizes:

Cylindrical charges of TNT explosive with masses from 100-3000g placed at standoff distances of 1m to 2m from Hardox plates.
Finite element models simulated in LS-DYNA based on LBE formulations to capture the detonation, blast wave propagation, and fluid-structure interaction with the Hardox plate.
By correlating the simulation results, the key relationships between charge size, standoff distance, reflected impulse parameters, and dynamic response of Hardox plates can be derived. This enables establishing damage and failure criteria for Hardox steels under extreme shock loading events.

**Finite Element Analysis**
Finite element analysis (FEA) simulations were performed in LS-DYNA to examine the response of Hardox plates when subjected to shockwave loading from explosive detonations. The Arbitrary Lagrangian Eulerian (ALE) method was utilized to model the surrounding air and propagation of the blast wave. The explosive charge was simulated using the *LOAD_BLAST_ENHANCED keyword, defined by the mass of TNT explosive and distance from the Hardox plate.
The material properties of the selected Hardox plate are as follows:

| RO-Mass Dnesity | E-Young Modulus | PR-Poisson Ratio | SIGY | ETAN-Tangent Modulus |
|---|---|---|---|---|
| 7800 | 2.00E+11 | 0.3 | 2.70E+08 | 1.00E+09 |

Figure3 illustrates the schematic of the experiment.

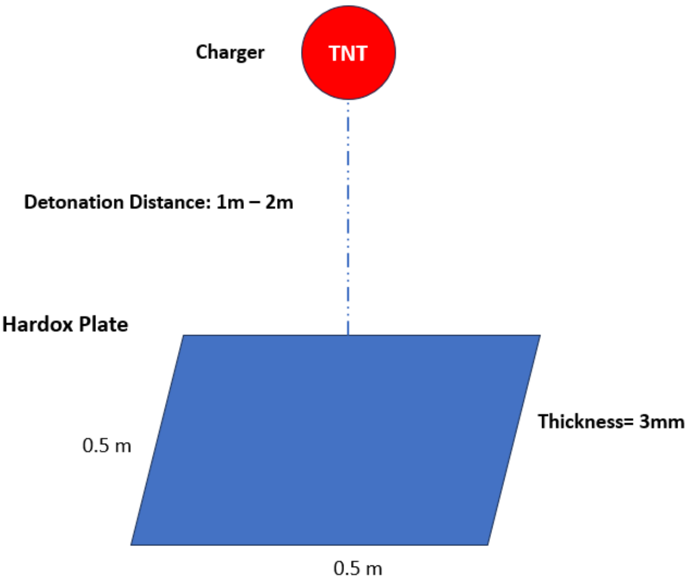


**Figure (3) Model of Hardox plate subjected to shock wave loading**

The FEA results provided insight into the deformation behavior and failure modes of the Hardox steel under extreme impulsive loading. As the blast wave impacts the plate, a high intensity compressive pressure wave is reflected, leading to plastic deformation. The center region of the plate experiences significant transverse deflection as it absorbs the impulse energy. For higher intensity explosions, petalling and rupture can occur due to excessive plastic strain localization. The impulse duration and peak pressure governed the extent of permanent plate deformation and potential cracking. By comparing FEA models with different standoff distances and charge sizes, the conditions under which Hardox plates undergo severe bruising, thinning, or fracture can be predicted. By comparing FEA models with different standoff distances and charge sizes, the conditions under which Hardox plates undergo severe bruising, thinning, or fracture can be predicted. This topic will be discussed in the next section.

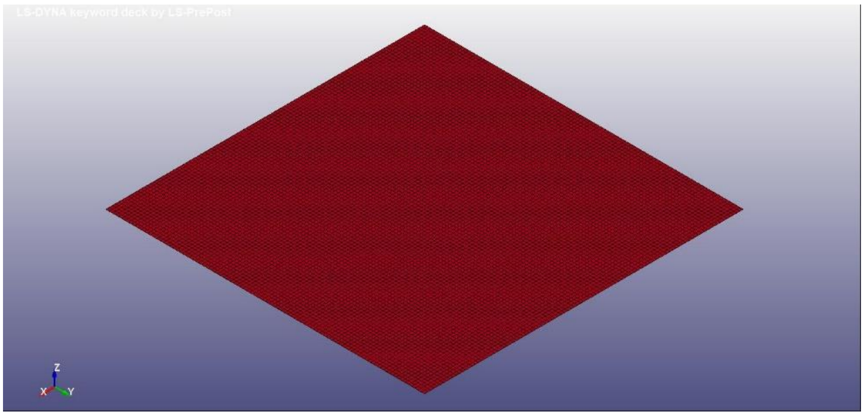


**Figure (3) LS-DYNA simulation of steel plates under shockwave loading**

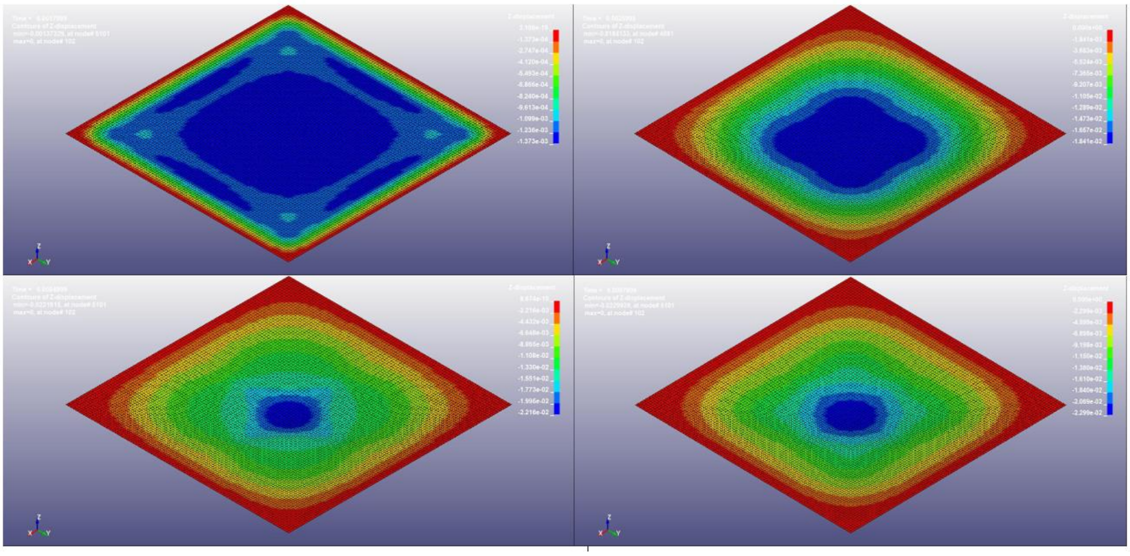

**Figure (4) Pressure Distribution on Hardox Plates under Shockwave Load**

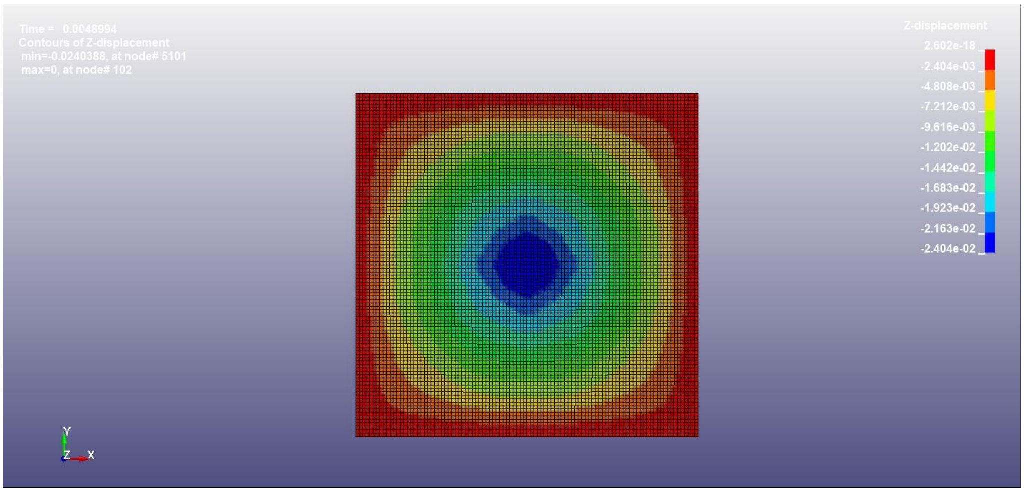

**Figure (5) Symmetrical nature of the problem under investigation**

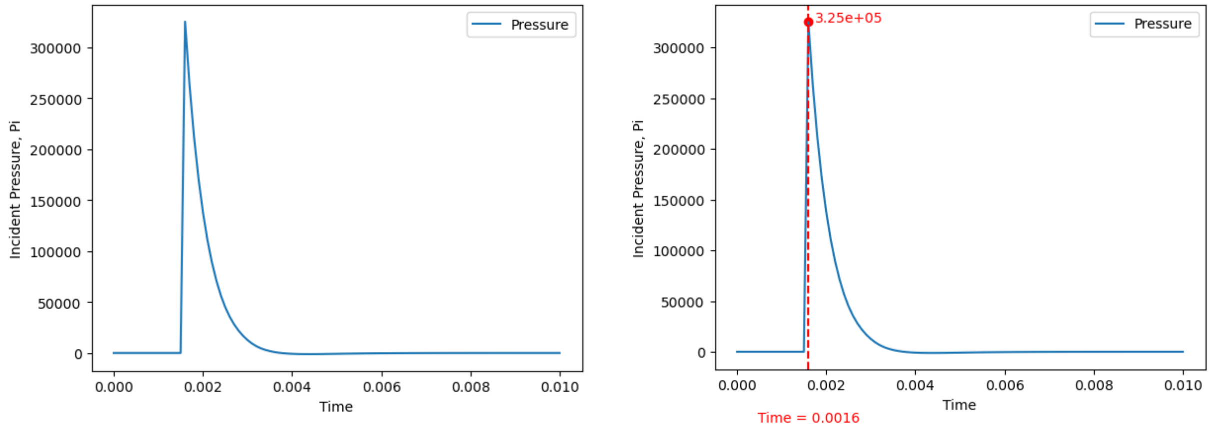


**Figure (6) Pressure-Time Profile of Hardox Plate Response to Shockwave loading- Mass of charger: 2kg, Size: 0.5*0.5, Thickness: 3mm**

The FEA methodology enabled Virtual testing of the Hardox materials under extreme shock loading scenarios difficult to replicate experimentally. The models provide greater understanding of the relationships between blast wave parameters and the dynamic response of Hardox over a wide range of strain rates. This supports development of more accurate material models for FEA and design guidelines to enhance the survivability and damage tolerance of Hardox steel components in blast or impact situations.

## Prediction of Hardox Plate Deflection

A Random Forest regression model was developed to predict the maximum deflection of Hardox plates subjected to shockwave loading from explosive detonations. The model was trained on a dataset of 300 simulations with the mass of TNT ranging from 100g to 3kg. The Hardox plate dimensions explored were 0.5m x 0.5m, 0.4m x 0.4m, and 0.3m x 0.3m. Plate thicknesses from 1mm to 3mm were analyzed. If the finite element simulation resulted in plate failure, indicated by a deflection over 0.05m, the model was provided this as a fail outcome.
The first 10 data from the Random Forest dataset are presented in Table 3.

**Table 3- Analytical Dataset for Predictive Modeling of Hardox Plate Deflection**

| Mass of TNT | Detonation Distance_m | Thickness_mm | Size_m | Maximum Deflection_m |
|---|---|---|---|---|
| 100 | 1 | 0.001 | 0.5 * 0.5 | 0.013473 |
| 200 | 1 | 0.001 | 0.5 * 0.5 | 0.013399 |
| 300 | 1 | 0.001 | 0.5 * 0.5 | 0.031476 |
| 400 | 1 | 0.001 | 0.5 * 0.5 | 0.038222 |
| 500 | 1 | 0.001 | 0.5 * 0.5 | 0.043802 |
| 600 | 1 | 0.001 | 0.5 * 0.5 | 0.050309 |
| 100 | 1 | 0.002 | 0.5 * 0.5 | 0.010894 |
| 200 | 1 | 0.002 | 0.5 * 0.5 | 0.014434 |
| 300 | 1 | 0.002 | 0.5 * 0.5 | 0.017707 |
| 400 | 1 | 0.002 | 0.5 * 0.5 | 0.020827 |

The dataset consisted of the TNT charge mass, plate dimensions, thickness, and the resulting peak deflection or fail condition from the simulations. 70% of the data was used for training while 30% was held out for testing model accuracy.

The Random Forest algorithm constructs an ensemble of decision trees, each built from a random subset of features. For this problem, the features were TNT mass, plate length, width, and thickness. The algorithm determines the split points and leaf nodes for each tree that best fit the training data. To make a prediction, the input features are propagated through each decision tree to obtain individual deflection predictions which are then averaged.

A grid search found the optimal hyperparameters as 150 trees and a maximum tree depth of 30. The trained Random Forest model achieved an R-squared of 0.97 and root-mean-square error is 0.00235 on the test set. This indicates the model accurately captures the relationship between blast parameters and Hardox deflection. The most important features were TNT mass and plate thickness.

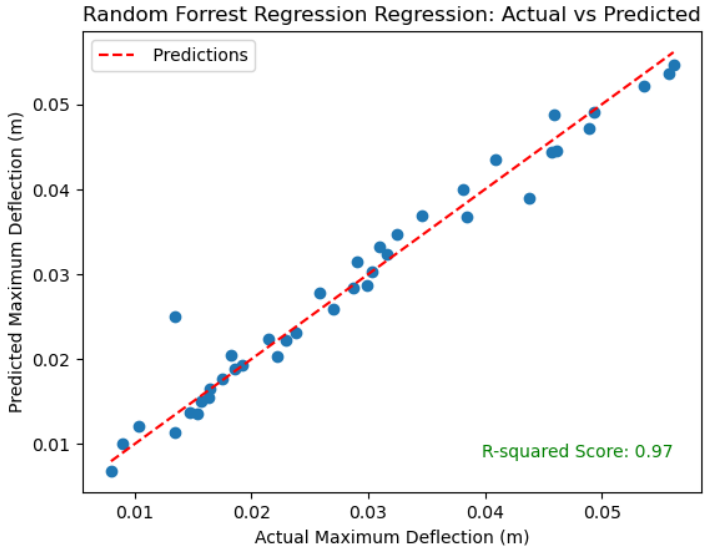


**Figure (7) Random Forrest Regression Accuracy**

While Random Forest Regression has demonstrated excellent performance for predicting the Maximum Deflection, we also explored the use of linear regression to understand the relationship between input features and the target variable. However, linear regression may not perform well when dealing with a complex and nonlinear problem.

Considering the limitations of linear regression in capturing the complexity of our problem, we propose a region-based approach. Initially dividing the dataset by sizes, subsequent classifications based on thickness and detonation distance will refine linear models for each subset. This method targets localized linear relationships within distinct regions, offering improved predictive accuracy where a global linear model may fall short. The approach enhances interpretability and allows tailored modeling for subsets with unique characteristics. Future steps involve fine-tuning region boundaries and evaluating the performance relative to the Random Forest Regression approach. A step-by-step description of the random forest algorithm is provided in the figure below.

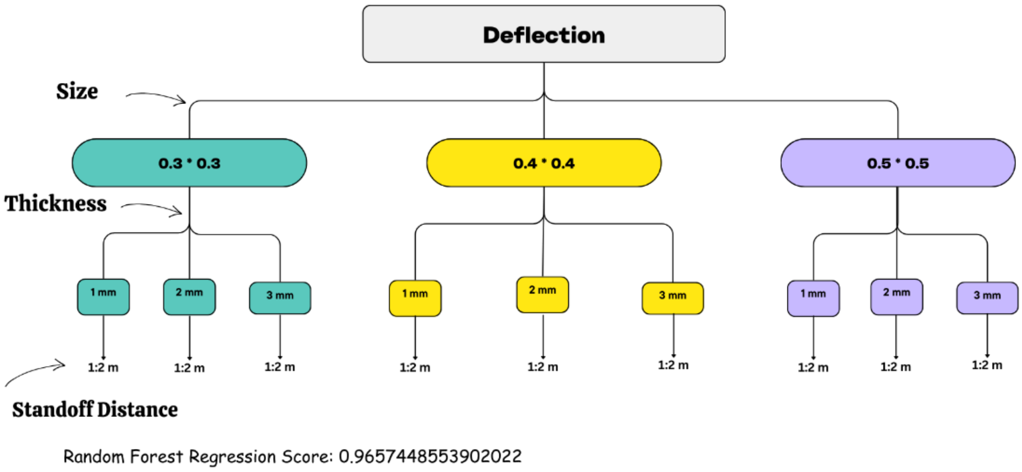


**Figure (8) Random Forest Algorithm**

Using the region-based approach, we can visualize linear regression on our dataset, which is shown in the figure below.

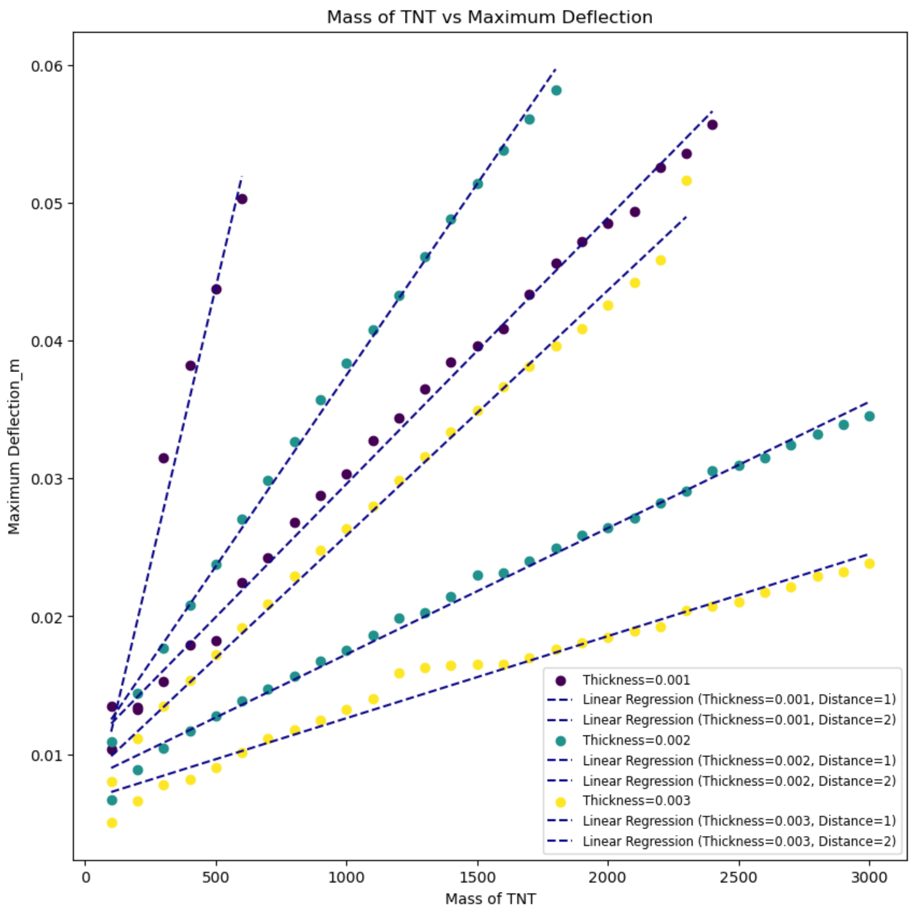


**Figure (9) Sequential Analysis- Classification Followed by Linear Regression**

The Random Forest model provides a rapid method to estimate Hardox plate deformations compared to finite element analysis. By interpolating results from simulations, reasonable deflection predictions are possible for untested combinations of plate parameters and charge sizes. This can assist designers in selecting appropriate plate dimensions and support structures when Hardox steel components are likely to experience extreme impulsive loading. The machine learning approach demonstrates the feasibility of data-driven models for predicting dynamic responses of materials.

**Conclusion**

This study investigated the dynamic response and deformation behavior of Hardox wear-resistant steel plates when subjected to extreme shockwave loading from explosive detonations. Controlled Shockwave experiments combined with finite element simulations provided insights into the performance of Hardox steels under high intensity impulsive loads.

The research found that key factors like peak incident pressure, impulse duration, and total imparted impulse govern the extent of plate deflection and potential for material failure. At moderate blast intensities, the exceptional hardness and strength of Hardox enables resisting significant bruising and plastic strains. However, excessive loading can lead to rupture, petalling, and fragmentation - as evidenced by the FEA models.

The machine learning model based on Random Forest regression demonstrated promising accuracy in predicting maximum deflection of Hardox plates for various combinations of blast parameters and plate thicknesses. This data-driven approach can assist designers in selecting appropriate dimensions and supports to enhance survivability of Hardox components that undergo extreme shocks in service.

Overall, this study enhanced fundamental understanding of the relationships between explosive blast characteristics and the dynamic response of hardened wear-resistant steels. The experimental data and simulation results will aid engineers in optimizing the thickness, joining, and mounting of Hardox parts intended for applications involving severe impacts. The analytical methodology and findings establish a framework to characterize the damage tolerance and failure mechanisms of quenched and tempered steels subjected to intense impulsive loads across a wide range of strain rates.

Future work should focus on validating the computational models with additional physical experiments. The deformation and cracking behavior of Hardox steels observed in this research can guide development of science-based injury and residual life assessment criteria for components subjected to extreme loading events. Extending the machine learning techniques to other scenarios and steel grades is recommended.

**References**

[1] Børvik, T., Dey, S., & Clausen, A. H. (2009). Perforation resistance of five different high-strength steel plates subjected to small-arms projectiles. International Journal of Impact Engineering, 36(7), 948-964.
[2] Hedjeres, S., Tria, D. E., Boudiaf, A., Kruszka, L., Hassani, S., & Alim, M. M. (2023). The influence of plasma nitriding hardness treatment on the dynamic compressive behavior of the Hardox 400 at a wide temperature range. Proceedings of the Institution of Mechanical Engineers, Part L: Journal of Materials: Design and Applications, 237(4), 867-885.
[3] Kharchenko, V., Kondryakov, E., Kravchuk, A., & Kotliarenko, A. (2022). Experimental and calculation investigations of deformation and fracture processes of various types of steels during impact shear tests. Procedia Structural Integrity, 36, 145-152.
[4] Mazur, M., & Mikova, K. (2016). Impact resistance of high strength steels. Materials Today: Proceedings, 3(4), 1060-1063.
[5] Dzioba, I., & Pała, R. (2019). Strength and fracture toughness of Hardox-400 steel. Metals, 9(5), 508
[6] “https://www.ssab.com/en/brands-and-products/hardox/product-program”.
[7] J. K. Xiao, H. Tan, J. Chen, A. Martini, and C. Zhang, “Effect of carbon content on microstructure, hardness and wear resistance of CoCrFeMnNiCx high-entropy alloys,” J. Alloys Compd., vol. 847, p. 156533, 2020, doi: 10.1016/j.jallcom.2020.156533.
[8] L. Chmielak, L. Mujica Roncery, P. Niederhofer, S. Weber, and W. Theisen, “CrMnFeCoNi high entropy

alloys with carbon and nitrogen: mechanical properties, wear and corrosion resistance," SN Appl. Sci., vol. 3, no. 11, 2021, doi: 10.1007/s42452-021-04814-y.

[9] Girault, E., Mertens, A., Jacques, P., Houbaert, Y., Verlinden, B., & Van Humbeeck, J. (2001). Comparison of the effects of silicon and aluminium on the tensile behaviour of multiphase TRIP-assisted steels. Scripta materialia, 44(6), 885-892.".

[10] Wang, W. F., & Wu, M. J. (2006). Effect of silicon content and aging time on density, hardness, toughness and corrosion resistance of sintered 303LSC–Si stainless steels. Materials Science and Engineering: A, 425(1-2), 167-171.".

[11] Wang, J., Lu, S., Rong, L., Li, D., & Li, Y. (2016). Effect of silicon on the oxidation resistance of 9 wt.% Cr heat resistance steels in 550 C lead-bismuth eutectic. Corrosion Science, 111, 13-25.".

[12] Huntz, A. M., Bague, V., Beauplé, G., Haut, C., Sévérac, C., Lecour, P., ... & Ropital, F. (2003). Effect of silicon on the oxidation resistance of 9% Cr steels. Applied Surface Science, 207(1-4), 255-275.".

[13] Mouayd, A. A., Koltsov, A., Sutter, E., & Tribollet, B. (2014). Effect of silicon content in steel and oxidation temperature on scale growth and morphology. Materials Chemistry and Physics, 143(3), 996-1004.".

[14] Nam, W. J., & Choi, H. C. (1999). Effect of Si on mechanical properties of low alloy steels. Materials science and technology, 15(5), 527-530.".

[15] Liu, J., Liu, W., Hao, Z., Shi, T., Kang, L., Cui, Z., & Yun, D. (2020). Effects of silicon content and tempering temperature on the microstructural evolution and mechanical properties of HT-9 steels. Materials, 13(4), 972.".

[16] De Moor, E., Speer, J. G., Matlock, D. K., Kwak, J. H., & Lee, S. B. (2011). Effect of carbon and manganese on the quenching and partitioning response of CMnSi steels. ISIJ international, 51(1), 137-144.".

[17] Dong, Q., Chen, X., Gao, Y., Hu, J., Chen, X., Xu, G. (2023). Steel. In: Dong, Q., Chen, X., Gao, Y., Hu, J., Chen, X., Xu, G. (eds) Civil Engineering Materials for Transportation Infrastructure. Springer, Singapore. https://doi.org/10.1007/978-981-99-130".

[18] Chen, XR., Zhai, QJ., Dong, H. et al. Molybdenum alloying in cast iron and steel. Adv. Manuf. 8, 3–14 (2020). https://doi.org/10.1007/s40436-019-00282-1".

[19] Tian, Y., Zhou, J., Shen, Y., Qu, Z., Xue, W., & Wang, Z. (2020). Improved toughness of a high-strength low-alloy steel for arctic ship by Ni and Mo addition. Advanced Engineering Materials, 22(6), 1901553.".

[20] Tian, Y., Ju, J., Fu, H. et al. Effect of Chromium Content on Microstructure, Hardness, and Wear Resistance of As-Cast Fe-Cr-B Alloy. J. of Materi Eng and Perform 28, 6428–6437 (2019). https://doi.org/10.1007/s11665-019-04369-5".

[21] Cruz, J. R., Henke, S. L., Pukasiewicz, A. G., & d'Oliveira, A. S. C. (2019). The effect of boron on cavitation resistance of FeCrMnSiB austenitic stainless steels. Wear, 436, 203041.".

[22] Cullis, I. G. (2001). Blast waves and how they interact with structures. BMJ Military Health, 147(1), 16.

[23] Ngo, T., Mendis, P., Gupta, A., & Ramsay, J. (2007). Blast loading and blast effects on structures–an overview. Electronic journal of structural engineering, (1), 76-91.

[24] Singh, A. K., Ditkofsky, N. G., York, J. D., Abujudeh, H. H., Avery, L. A., Brunner, J. F., ... & Lev, M. H. (2016). Blast injuries: from improvised explosive device blasts to the Boston Marathon bombing. Radiographics, 36(1), 295-307.

[25] Bhatti, A. Q., Badshah, E., Naseer, A., Ashraf, M., Shah, F., & Akhtar, K. (2017). Review of blast loading models, masonry response, and mitigation. Shock and Vibration, 2017, 6708341.

[26] Shirbhate, P. A., & Goel, M. D. (2021). A critical review of blast wave parameters and approaches for blast load mitigation. Archives of Computational Methods in Engineering, 28, 1713-1730.